Dissolved organic matter enhanced the aggregation and oxidation of nanoplastics under simulated sunlight irradiation in water

Zhang, Y.N.; Cheng, F.Y.; Zhang, T.T.; Li, C.; Qu, J.; Chen, J.W.; Peijnenburg, W.J.G.M.

Environmental Science & Technology

pubs.acs.org/est

Article

Dissolved Organic Matter Enhanced the Aggregation and Oxidation of Nanoplastics under Simulated Sunlight Irradiation in Water

Ya-nan Zhang, Fangyuan Cheng, Tingting Zhang, Chao Li, Jiao Qu,* Jingwen Chen, and Willie J. G. M. Peijnenburg

Cite This: *Environ. Sci. Technol.* 2022, 56, 3085−3095

Read Online

ACCESS | Metrics & More | Article Recommendations | Supporting Information

ABSTRACT: Nanoplastics (NPs) have become a new type of pollutant of high concern that is ubiquitous in aqueous environments. However, the transport and transformation of NPs in natural waters are not yet fully understood. In this study, the aggregation and photooxidation of NPs were assessed with nanosized polystyrene (PS) as an example, and the effects of dissolved organic matter (DOM) were investigated with Suwannee River fulvic acid (SRFA) as representative DOM. The results showed that simulated sunlight irradiation exhibited negligible effects on the aggregation of PS, while SRFA enhanced its heteroaggregation through hydrophobic interactions. In SRFA solutions, photooxidation of PS with a particle size of 200 nm was observed, which led to an increase in the O/C ratio on its surface at a rate of $(2.20 \pm 0.40) \times 10^{-2}$ h^{-1}. This indicates the promotional effect of SRFA on the oxidation of nanosized PS, which is attributed to the generation of the excited triplet state (^{3}SRFA*), hydroxyl radicals ($^\bullet$OH), and singlet oxygen ($^1O_2$). Among these reactive species, $^1O_2$ played a crucial role in the oxidation of PS. The findings in this study are helpful for an in-depth understanding of the environmental behavior of NPs in natural waters.

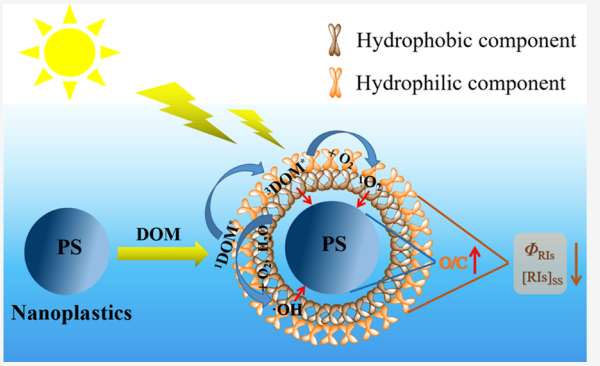

KEYWORDS: *nanoplastics, aggregation, photooxidation, dissolved organic matter, photochemically produced reactive intermediates*

INTRODUCTION

In recent years, plastics have attracted much attention as a class of emerging pollutants.[1−4] An increasing mass of plastics has been detected in surface waters around the world due to the increasing discharge of plastic waste.[5−7] Among the various plastics present, polypropylene (PP), poly(vinyl chloride) (PVC), polystyrene (PS), and polyethylene (PE) are commonly detected in surface waters.[6,8] Increasing research is currently focused on the distribution and environmental behavior of these plastics in water systems.[9,10]

A large number of plastics exhibit toxic effects on organisms and may cause serious ecological risks. Studies on the toxicological effects of plastics showed that ingestion of microplastics (MPs, <5 mm in diameter) and nanoplastics (NPs, <1 μm in diameter) by animals can induce damage to their reproductive ability and to specific organs,[9,11] whereas NPs were found to penetrate cell walls and reach the circulatory system.[12] At the same time, MPs can also affect the transport behavior of organic pollutants in the environment.[9] They have been reported to be carriers of various contaminants in natural waters due to the strong adsorption ability of hydrophobic organic pollutants, such as polychlorinated biphenyls (PCBs), polycyclic aromatic hydrocarbons (PAHs), and per- and polyfluorinated chemicals (PFCs).[13−16] Thus, it is of great significance to understand the transport and degradation behavior of plastics in natural waters to be able to properly assess their potential ecological risks. However, less attention has been given to the transport and degradation of NPs in natural waters compared with those of MPs.

The main environmental fate-determining processes of plastics in natural waters are aggregation and degradation, including photodegradation, thermal degradation, biodegradation, and oxidation reactions.[4,17,18] These processes may alter the properties of plastics, including their size, morphology, mechanical strength, and oxygen content.[19−21] The aggregation of plastics, e.g., MPs, in natural waters is likely to be affected by dissolved organic matter (DOM), which is a ubiquitous natural organic macromolecule in aquatic ecosystems.[22] Previous research has shown that DOM can affect the environmental behavior of nanoparticles,[23] and heteroaggregation was proven to occur in the presence of DOM due to electrostatic repulsion and hydrophobic interactions, thereby changing the fate and distribution of nanoparticles in the

Received: October 19, 2021
Revised: February 4, 2022
Accepted: February 7, 2022
Published: February 17, 2022

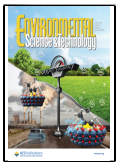

aquatic environment.[23] As a kind of nanoparticle, the surface morphology and fate of NPs can also be affected by DOM. The aggregation of MPs was proven to be affected by DOM and ionic strength, and the heteroaggregation of MPs was reported to change in the presence of inorganic colloids and natural organic matter.[24,25] However, in sunlit surface water, the influence of DOM on the aggregation of NPs is still unclear.

Under long-term irradiation in water, the surface properties and microstructure of MPs, such as color, surface morphology, and density, can be changed.[26−28] In addition, photochemically produced reactive intermediates (PPRIs), such as singlet oxygen ($^1O_2$) and hydroxyl radicals ($^•OH$), can react on the surface of MPs to accelerate their photodegradation in natural waters.[26,27] The reaction of $^1O_2$ and $^•OH$ with MPs can lead to the formation of oxygen-containing functional groups on the surface of MPs and can enhance their negative surface potential in water,[26,29] which subsequently affects their fate and transport, as well as their potential risks in the environment.[30−33] In estuarine water and coastal seawater, the presence of Cl^- can inhibit the photooxidation of MPs by generating $Cl_2^{•-}$.[27] DOM has been proven to play an important role in photochemical processes in aquatic environments.[34,35] Upon irradiation, DOM can generate various photochemically produced reactive intermediates (PPRIs), such as the excited triplet state of DOM (^{3}DOM*), $^1O_2$, and $^•OH$.[36,37] Thus, DOM may also influence the degradation behavior of NPs in sunlit surface waters. Nevertheless, sunlight-induced degradation of NPs in the presence of DOM and the roles of PPRIs in the photodegradation of NPs are still unclear. In addition, NPs at environmentally relevant concentrations can interact with DOM[38] and induce structural changes in DOM.[24] Thus, the interaction of DOM with NPs may affect the generation of PPRIs from DOM, which can influence the photodegradation of various pollutants, including particles, initiated by these PPRIs.[35,39]

Once released into natural water, NPs have great potential to interact with DOM, which has a significant impact on the environmental fate of NPs. Thus, in this study, the predominant aim was to investigate the aggregation and photooxidation behaviors of NPs under simulated sunlight irradiation and to reveal the mechanisms related to the interaction of DOM with NPs affecting the behavior of NPs. Nanosized PS and Suwannee River fulvic acid (SRFA) were selected as representatives of NPs and DOM, respectively. The obtained results could increase our understanding of the environmental behavior of NPs and provide new scientific evidence for the potential risks of NPs in natural waters.

MATERIALS AND METHODS

Chemicals. PS suspensions (50 mg/mL density: 1.05 g/cm^3; solvent: ultrapure water; and no group modification on the surface of PS) with particle sizes of 50, 200, and 1000 nm were purchased from Zhongkeleiming Technology Co., Ltd. (Beijing, China). 2,4,6-Trimethylphenol (TMP, 98%), furfuryl alcohol (FFA, 98%), sorbic acid (SA, 99% purity), benzene (99%), and phenol (99%) were purchased from J&K Scientific, Ltd. (Beijing, China). Suwannee River fulvic acid Standard II (SRFA, 2S101F) was purchased from the International Humic Substances Society. Sodium dihydrogen phosphate (NaH_2PO_4) and disodium hydrogen phosphate (Na_2HPO_4) were purchased from Tianjin Damao Chemical (Tianjin, China). Ultrapure water (18.2 MΩ) was obtained from a purification system produced by Chengdu Ultrapure Technology Co., Ltd. (Chengdu, China). The organic solvents used in this study were of chromatographical purity and were obtained from TEDIA (Fairfield, OH).

The PS suspensions were diluted with pure water to a final concentration of 200 mg/L and subsequently used as PS stock solutions. Appropriate amounts of SRFA in deionized water were dissolved and filtered with 0.45 μm of poly(vinylidene fluoride) to prepare a 1 g/L stock solution.

Oscillation Experiments. Oscillation experiments were performed to investigate the aggregation of PS with particle sizes of 50, 200, and 1000 nm in an aqueous environment. Micron-sized PS (1000 nm, i.e., 1 μm) was selected as a control of MPs. PS with an initial concentration of 20 mg/L was placed in a conical flask, and phosphate buffer solution (PBS, 1.0 mM) was used to control the pH of the solutions at 7.0. The solutions were oscillated in a constant-temperature oscillator under dark conditions for 7 days (25 ± 1 °C, 150 rpm) as described in a previous study in which the interaction equilibrium time of PS with humic acid was approximately 7 days.[24] Samples were collected at predetermined time intervals (0, 1, 2, 3, 4, 5, 6, and 7 days) for the determination of average hydrodynamic diameters. In addition, their morphology and microstructure were observed, and the elemental composition (C and O) on the surface of PS was determined.

The effect of DOM on the aggregation of PS was investigated by adding SRFA (10 mg/L) to PBS solutions, and the influence of simulated sunlight irradiation on the aggregation of PS was also investigated with the detailed irradiation methods shown below. All experiments were conducted in triplicate.

Light Irradiation Experiments. The irradiation experiments were carried out in an XPA-7 merry-go-round photochemical reactor (Xujiang Electromechanical Plant, Nanjing, China) with quartz tubes containing the reaction solutions. A water-refrigerated 500 W medium-pressure mercury lamp equipped with 290 nm filters (λ > 290 nm) was used to mimic the UV-A and UV-B portions of sunlight. The light intensity at the surface of the quartz tubes was detected with a TriOS-RAMSES spectroradiometer (TriOS GmbH, Germany), and the results are shown in Figure S1 in the Supporting Information (SI). During irradiation, a circulating cooling water system was used to keep the temperature at 25 ± 1 °C, which could not change the physical and chemical properties of PS.[40] A magnetic stirring system at a speed of 700 rpm was used to keep PS and SRFA fully mixed in the suspensions and to simulate the mechanical abrasion forces in natural waters.[27]

The influence of light irradiation on the aggregation of PS was investigated. During light irradiation, samples were collected at predetermined time intervals (0, 10, 30, 50, 80, and 120 min), and the ζ-potential and average hydrodynamic diameter of PS were determined. In addition, the effect of light irradiation on the aggregation of PS that had been oscillated for 7 days was also observed.

Photodegradation experiments were carried out to investigate the photooxidation of PS. Different particle sizes (200 and 1000 nm) of PS with an initial concentration of 20 mg/L and SRFA (10 mg/L) were thoroughly mixed in PBS (1.0 mM, pH = 7.0). Although the actual estimated average concentration of MPs is <1 mg/L in natural waters,[41] relatively higher concentrations of NPs were used because the concentrations of NPs in natural waters are considered to be much higher than

https://doi.org/10.1021/acs.est.1c07129
Environ. Sci. Technol. 2022, 56, 3085−3095

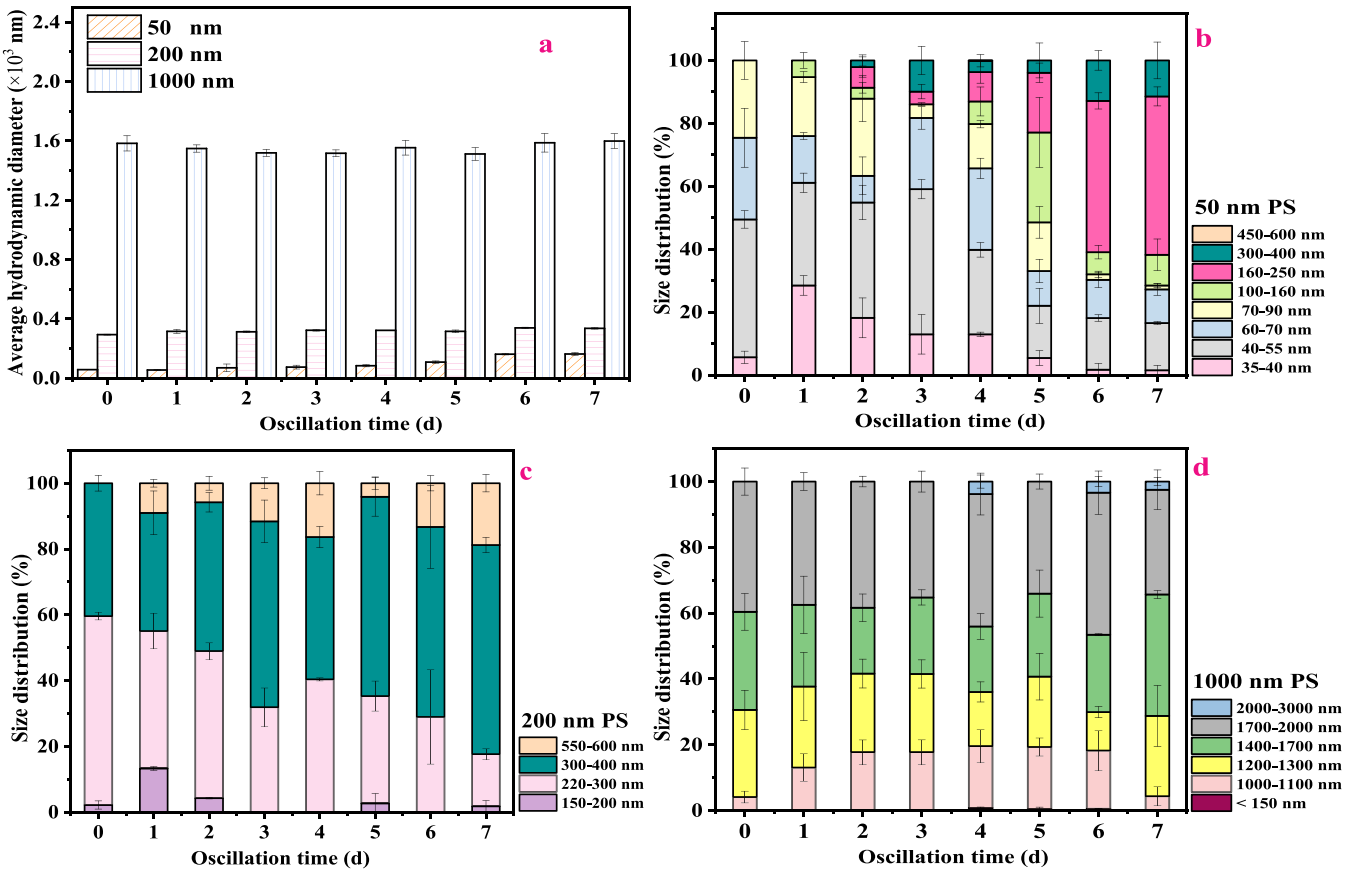

Figure 1. Average hydrodynamic diameters (a) and particle size distribution (b, c, d) of PS (20 mg/L) during 1 week of oscillation (oscillation conditions: 150 rpm, 25 °C).

those of MPs[42] and the higher concentration of NPs is helpful to facilitate instrumental analysis.

The samples were oscillated for 1 week in a constant-temperature oscillator (25 ± 1 °C, 150 rpm) to ensure the interaction equilibrium of PS and SRFA, and the irradiation experiment was carried out subsequently. The samples containing only PS or SRFA were treated as blank controls. Photodegradation experiments were performed with predetermined time intervals (0, 2, 4, 8, 16, and 24 h), and the elemental composition (C and O) on the surface of PS was determined after pretreatment.

SA (5 mM), isopropyl alcohol (IPA, 20 mM), and FFA (1 mM) were used as quenchers for ^{3}DOM*, $^\bullet$OH, and $^1O_2$, respectively,[43−46] and were used to reveal the roles of ^{3}DOM*, $^1O_2$, and $^\bullet$OH produced by SRFA in the photooxidation of PS. All experimental conditions were conducted in triplicate.

Determination of PPRIs from SRFA. TMP, FFA, and benzene were used as probe chemicals to measure the apparent quantum yields (Φ) and steady-state concentrations of ^{3}DOM*, $^1O_2$, and $^\bullet$OH, respectively.[47−50] The calculation methods of the steady-state concentrations and Φ of ^{3}DOM* ($[^3DOM^*]_{SS}$), $^1O_2$ ($[^1O_2]_{SS}$), and $^\bullet$OH ($[^\bullet OH]_{SS}$) are detailed in Text S2.

The effect of PS on the generation of these PPRIs from SRFA (10 mg/L) was investigated by adding PS (50 nm) at different concentrations (0.5, 5, 10, and 20 mg/L) or PS (20 mg/L) with different particle sizes (50, 200, and 1000 nm) in PBS (1.0 mM, pH = 7.0). The role of oscillation on the generation of these PPRIs from SRFA was investigated by performing irradiation experiments with samples oscillated for 7 days. During light irradiation, samples were collected at predetermined time intervals (0, 10, 30, 50, 80, and 120 min) and filtered with 0.45 μm of poly(vinylidene fluoride) for subsequent analysis. All experimental conditions were conducted in triplicate.

Sample Pretreatment and Analytical Methods. The ζ-potential and average hydrodynamic diameter of PS were measured by dynamic light scattering (DLS) using a Zetasizer ZS (Malvern, U.K.). The samples were obtained during oscillation or irradiation treatment, and the solution was placed in a sample cell for measurement using a He−Ne laser operating at a wavelength of 633 nm and a scattering angle of 90°.

The morphology and microstructure of PS during the treatment were characterized by field emission scanning electron microscopy (FE-SEM, HITA CHIS-4800). The samples were obtained and directly dropped onto monocrystalline silicon sheets (1 cm × 1 cm). The samples were completely dried in a vacuum-drying oven at 60 °C, and SEM analysis at acceleration voltages of 15.0−25.0 kV was performed after spraying gold.

The elemental composition (C and O) on the surface of PS during the treatment was determined by field emission scanning electron microscopy (FE-SEM, HITA CHIS-4800) coupled with energy-dispersive spectrometry (EDS). The detailed methods are as follows: 25 mL of samples were collected and centrifuged at high speed several times (15 000 rpm, 20 min) to remove the aqueous phase and to collect the PS precipitate from the bottom of the centrifuge tube.[24] Then,

https://doi.org/10.1021/acs.est.1c07129
Environ. Sci. Technol. 2022, 56, 3085−3095

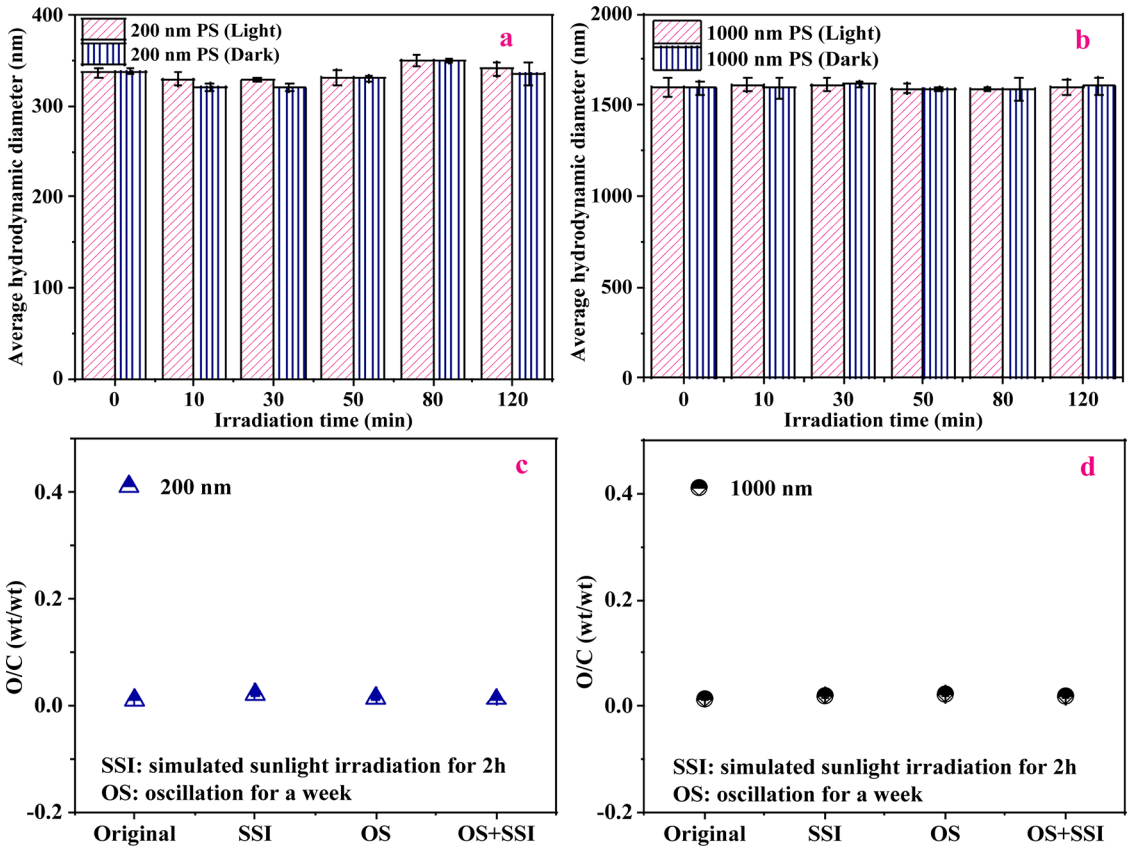

Figure 2. Average hydrodynamic diameters of PS (20 mg/L) during simulated sunlight irradiation after 1 week of oscillation (a, b) and the O/C ratio (wt/wt) of PS after treatment with oscillation and light irradiation (c, d). Oscillation conditions: 150 rpm, 25 °C.

5 mL of ultrapure water was added to the centrifuge tube containing the PS precipitate, and the solution was vortexed for 5 min. The cleaning process was repeated three times to remove the SRFA adsorbed on the surface of PS. Finally, the collected precipitate was dropped on a monocrystalline silicon sheet (1 cm × 1 cm) with a glass dropper and dried in a vacuum-drying oven at 60 °C until completely dried. EDS was used to measure the O/C content on the PS surface after gold spraying.

An Agilent 1260 II HPLC system (Agilent) with a UV−vis detector and an Ultimate AQ-C18 column (250 mm × 4.6 mm, 5 mm, Welch Materials, Maryland) was employed for the quantification of TMP, FFA, and phenol, as detailed in Table S1.

RESULTS AND DISCUSSION

Aggregation and Degradation of PS during Oscillation and Light Irradiation. The morphology and microstructure of PS during oscillation and light irradiation were observed using SEM, and the results are shown in Figure S2. The original PS particles had smooth and globular features (Figure S2a), and the polymer dispersity index (PDI) was very small (<0.1, Table S2), indicating that the size distribution was uniform.[51] The average hydrodynamic diameters of PS during oscillation were measured to investigate the aggregation of PS, and the results are shown in Figure 1. The determined values of the average hydrodynamic diameter of PS were higher than the theoretical values (50, 200, and 1000 nm) due to its slight agglomeration of PS in aqueous solutions. Aggregation of PS with a particle size of 50 nm was observed during 1 week of oscillation as the average hydrodynamic diameter increased during the oscillation (Figure 1a). Although no obvious increase in the average hydrodynamic diameter was observed for PS with particle sizes of 200 and 1000 nm, slight aggregation occurred as the ratio of large PS particles increased during oscillation (Figure 1b−d).

Compared with the untreated 1000 nm PS, the oscillation-treated PS was obviously ruptured (Figure S2b), and lower particle-sized PS (<150 nm) was detected during oscillation (Figure 1d). This indicates that the oscillation of PS could lead to the generation of PS fragments of lower particle size. Thus, it can be concluded that the mechanical abrasion forces brought about by the fluctuation of the water flow have an important effect on the surface aging of PS particles with large particle sizes, which is in accordance with a previous study.[52] This leads to the breaking and cracking of microscale particles into nanoscale plastics. Therefore, the abundance of NPs in natural waters may be far underestimated, especially upon prolonged emissions of MPs in the aquatic environment.

No significant increase in the average hydrodynamic diameter (Figures 2a,b and S3) and no obvious change in the particle size distribution (Figure S4) were observed for PS particles with different particle sizes (50, 200, and 1000 nm) no matter during simulated sunlight irradiation directly or during irradiation after 1 week of oscillation. These results demonstrated that simulated sunlight irradiation exhibited a negligible effect on the aggregation of PS, which is in accordance with the observed dispersion state of PS in the SEM images (Figure S2).

https://doi.org/10.1021/acs.est.1c07129
Environ. Sci. Technol. 2022, 56, 3085−3095

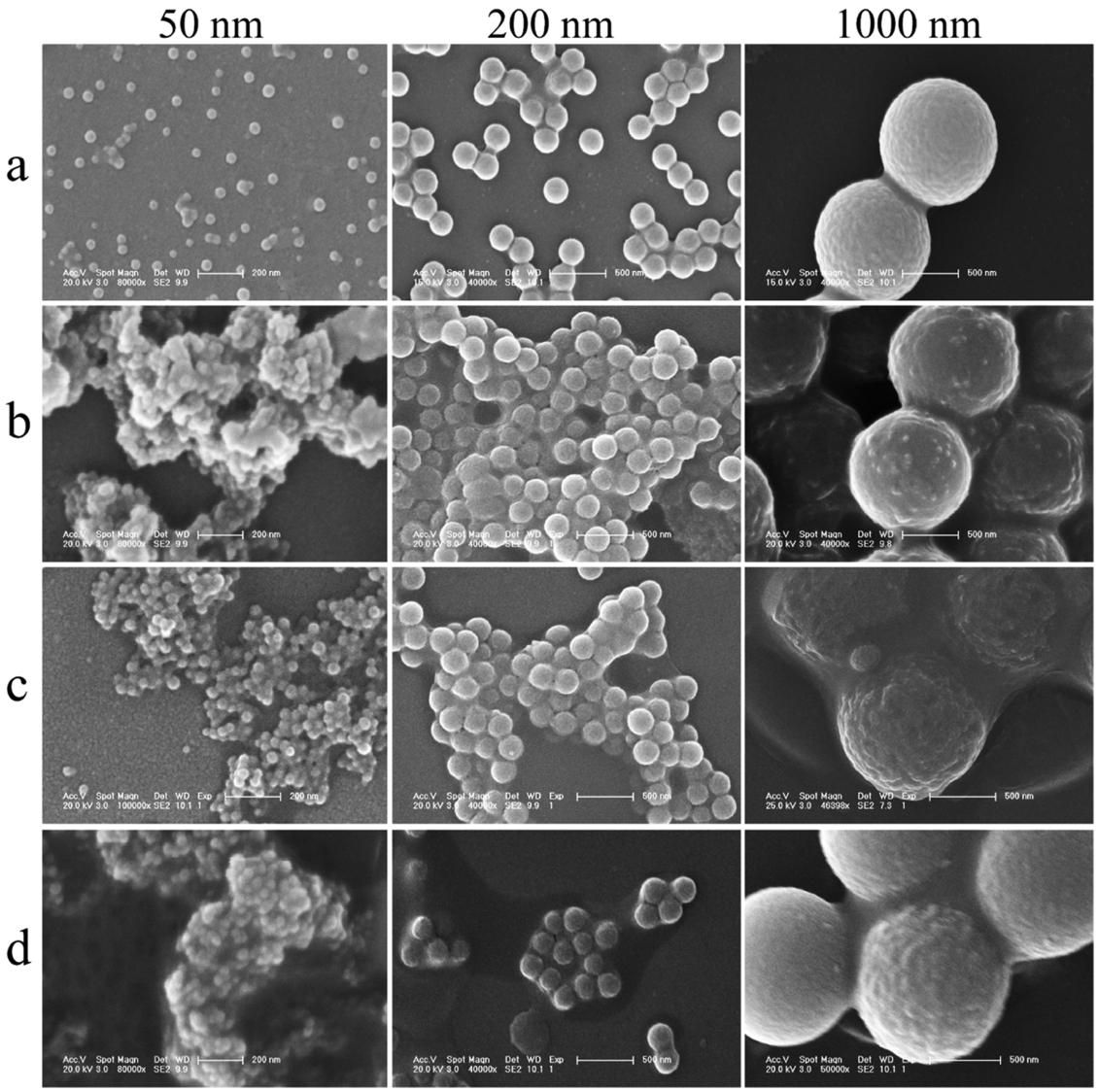

Figure 3. SEM images of initial PS (a), PS after 1 week of oscillation (b), PS after 2 h of light irradiation with (c) and without 1 week of oscillation (d) in the presence of SRFA (oscillation conditions: 150 rpm, 25 °C; PS: 20 mg/L; and SRFA: 10 mg/L).

The elemental composition (C and O) on the surface of PS with particle sizes of 200 and 1000 nm was analyzed, and the O/C ratio (wt/wt) was calculated. There was 1.08 and 1.30% O (wt %) in the original PS with particle sizes of 200 and 1000 nm, respectively, which is attributed to the gold-spraying process during the pretreatment of samples for EDS analysis. No obvious changes in the O/C ratio for PS were observed after simulated sunlight irradiation, oscillation, and a combination of oscillation followed by irradiation (Figure 2c,d). Thus, it can be concluded that direct irradiation cannot induce the oxidation of nanoscale PS in sunlit surface waters.

Influence of SRFA on Aggregation of PS. In the presence of SRFA, SEM images of PS with different particle sizes after treatment with oscillation and/or light irradiation are shown in Figure 3. In the presence of SRFA, slight aggregation of PS was observed (Figure 3a), indicating the promotional effect of SRFA on the aggregation of PS. After 1 week of oscillation, a stronger interaction between PS and SRFA was observed compared with that without SRFA (Figures 3b vs S2b). Thus, heterogeneous aggregation between PS and SRFA occurred in this system. After 1 week of oscillation, simulated sunlight irradiation showed no obvious effect on the dispersion state of PS in the presence of SRFA after oscillation (Figure 3c vs 3b), which also confirmed the negligible effect of simulated sunlight irradiation on the aggregation of PS particles. After light irradiation without oscillation, slight aggregation of PS was also observed (Figure 3d), which is attributed to 2 h stirring during the simulated sunlight irradiation.

SRFA contains multiple functional groups and organic components, such as humic acid-like and fulvic acid-like components.[53] The interaction with SRFA molecules (such as intramolecular energy transfer, excited-state electron transfer, and charge transfer)[54−56] may affect the surface charge of PS, and the neutralization of positive and negative charges in the solution could lead to the appearance of the isoelectric point, which is a preferable condition for the formation of large heterogeneous aggregates of NPs.[23,25] Therefore, the ζ-potential at the PS surface was measured during oscillation and light irradiation. The initial ζ-potentials of 50, 200, and 1000 nm of PS were −38.15, −12.43, and −24.50 mV, respectively (Table S2).

https://doi.org/10.1021/acs.est.1c07129
Environ. Sci. Technol. 2022, 56, 3085−3095

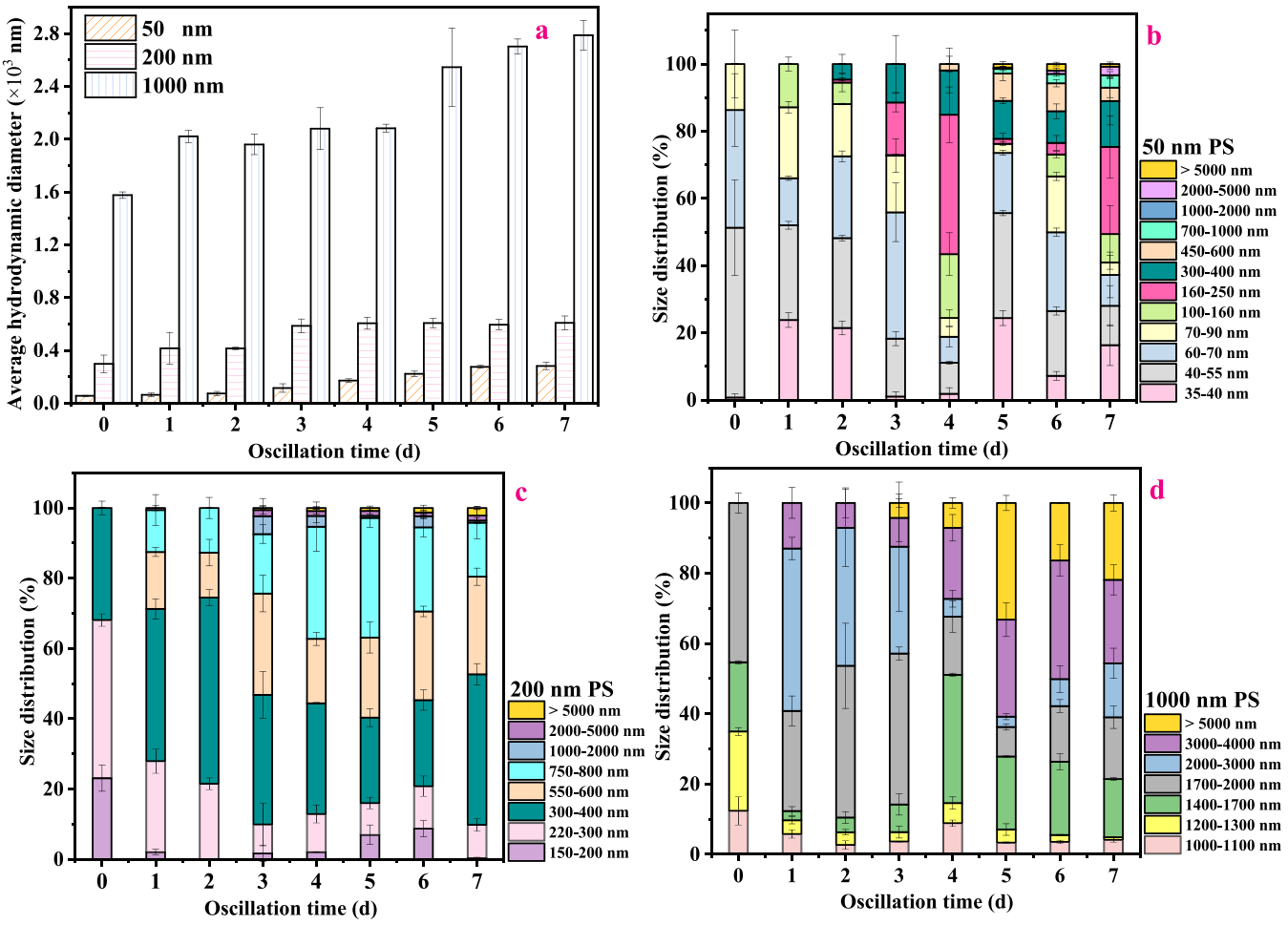

Figure 4. Average hydrodynamic diameters (a) and particle size distribution (b, c, d) of PS during 1 week of oscillation in the presence of SRFA (oscillation conditions: 150 rpm, 25 °C; PS: 20 mg/L; and SRFA: 10 mg/L).

No obvious change in the ζ-potential of PS with each particle size was observed in the presence of SRFA during 1 week of oscillation (Figure S5). Therefore, the electrostatic interaction during the oscillation process was not the reason for the heteroaggregation of PS and SRFA. There are hydrophobic acids in SRFA,[53] indicating the presence of hydrophobic domains that can serve as aggregation points for the assembly of SRFA and PS. This indicates that hydrophobic interactions play important roles in the adsorption of PS and SRFA. Moreover, no significant change in the ζ-potential of PS was observed during the light irradiation directly or during irradiation after 1 week of oscillation (Figure S5), indicating that simulated sunlight irradiation has little effect on the charge distribution of PS in SRFA solutions.

The average hydrodynamic diameters and the particle size distribution of PS during oscillation and light irradiation were measured to investigate the aggregation of PS in the presence of SRFA, and the results are shown in Figures 4, S6, and S7. The results showed that the average hydrodynamic diameter of PS particles increased during 1 week of oscillation in the presence of SRFA (Figure 4a), and the increase was much higher than that without SRFA (Figure 1a). These results demonstrated the promotional effect of SRFA on the aggregation of nanosized PS. In the presence of SRFA, the contribution of large-sized particles significantly increased during oscillation (Figure 4b–d), which also confirms the enhanced aggregation of PS induced by SRFA. The aggregation effect increased with decreasing particle size, which is consistent with the results in previous research.[24] During light irradiation with and without 1 week of oscillation, no significant changes in the average hydrodynamic diameters and the particle size distribution of PS in the presence of SRFA were observed compared with the dark controls (Figures S6 and S7), which also confirmed the negligible role of direct light irradiation on the aggregation of PS.

Small-sized particles (<150 nm) were detected (Figure 1d), and cracks were observed (Figure S2b) in PS with an initial particle size of 1000 nm during 1 week of oscillation, but these phenomena were not observed in the SRFA solution (Figures 3b and 4d). This indicates that the coating of SRFA on the PS surface has a protective effect. It has been reported that DOM can be coated on nanoparticles to form a relatively stable complex.[22] Thus, DOM could act as a protector against the fracture of MPs into NPs in natural waters. The hydrophobic forces and $\pi-\pi$ interactions between DOM and PS were supposed to be the main reasons for heteroaggregation.[23,38] Hence, DOM in the environment has important impacts on the dispersibility of MPs, especially NPs with a smaller particle size, which further affects their fate in natural waters, as well as their environmental risks.

Effect of SRFA on Photooxidation of PS. During the photooxidation process, reactive oxygen species (ROS)-

https://doi.org/10.1021/acs.est.1c07129
Environ. Sci. Technol. 2022, 56, 3085−3095

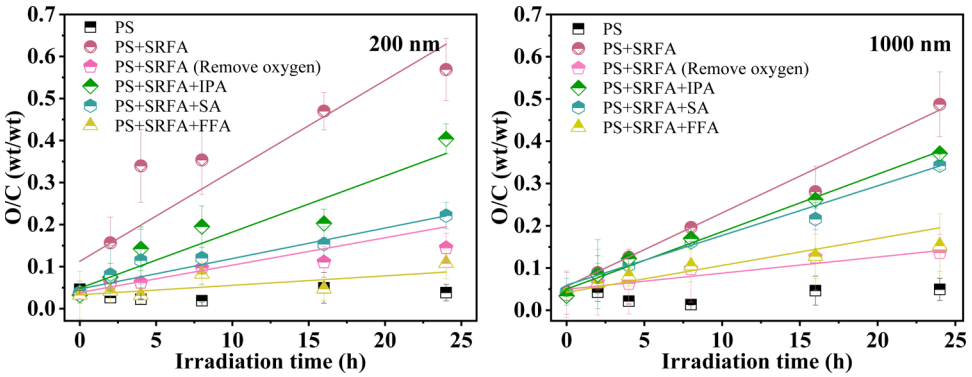

Figure 5. O/C ratio on the PS surface during simulated sunlight irradiation after 1 week of oscillation (oscillation conditions: 150 rpm, 25 °C; PS: 20 mg/L; SRFA: 10 mg/L; IPA: isopropyl alcohol, 20 mM; SA: sorbic acid, 5 mM; and FFA: furfuryl alcohol, 1 mM).

initiated reactions could lead to an increase in the oxygen content on the surface of plastics.[26,57,58] SRFA can produce PPRIs such as the excited triplet states of SRFA (^{3}SRFA*), $^1O_2$, and $^\bullet$OH under simulated sunlight irradiation, which may affect the photodegradation of PS in surface waters. Thus, EDS was used to analyze the elemental composition of PS particles, and the results are shown in Figures S8 and S9 in the SI. The oxygen/carbon ratio (O/C) was calculated and used to evaluate the degree of oxidation of PS under simulated sunlight irradiation. The oxidation rate of PS was obtained by fitting the O/C ratio versus irradiation time, and the results are shown in Table S3 in the SI.

Compared with the control samples (PS), the addition of SRFA significantly enhanced the oxidation reaction of PS particles of different sizes (Figure 5) after 1 week of oscillation, and no obvious changes in the average hydrodynamic diameters of PS were observed (Figure S10). As shown in Figure 5, the O/C on the surface of PS increased significantly during simulated sunlight irradiation in the presence of SRFA with oxidation rates of $(2.20 \pm 0.40) \times 10^{-2}$ h^{-1} and $(1.74 \pm 0.11) \times 10^{-2}$ h^{-1} for 200 and 1000 nm PS, respectively. The O/C of PS with sizes of 200 and 1000 nm increased from 0.03 and 0.04 to 0.56 and 0.48, respectively, within 24 h of irradiation. Moreover, the oxidation rate of PS with a nominal size of 200 nm was higher compared with the oxidation rate of PS particles with a diameter of 1000 nm (Figure 5 and Table S3 in the SI). This finding indicates a stronger effect of SRFA on the degradation/oxidation of PS particles with smaller particle sizes, which is in accordance with the higher promotional effect of SRFA on the aggregation of PS with small particle sizes (Figure 4). No obvious change in the O/C of PS was observed during the irradiation process without SRFA (Figure 2). Additionally, the high-speed centrifugal elution process had no effect on the O/C of the PS surface (Figure S8). It can thus be concluded that the oxidation of PS is mainly attributable to the indirect photodegradation initiated by the PPRIs derived from SRFA.

To further understand the mechanisms by which SRFA influences the photooxidation of PS, quenching experiments were carried out. The results of these experiments are shown in Figure 5. The addition of SA significantly decreased the O/C of PS, implying that ^{3}SRFA* is involved in the oxidation of PS. Previous studies have proven that the reaction of ^{3}DOM* with dissolved oxygen in water leads to the generation of $^1O_2$ through energy transfer and the formation of $^\bullet$OH through electron transfer.[47,48] Thus, the samples were saturated with nitrogen to remove dissolved oxygen. The results of this experiment showed that the O/C of PS was significantly reduced compared with the O/C in SRFA only and in the presence of SA. This indicates a more important role of $^1O_2$ and/or $^\bullet$OH in the oxidation of PS compared with ^{3}SRFA*. The involvement of $^1O_2$ and $^\bullet$OH in the photodegradation of MPs was observed in a previous study,[26] which could lead to an increase in the O/C ratio on the surface of MPs during advanced oxidation processes.[29]

The role of $^1O_2$ and $^\bullet$OH in the oxidation of PS was further investigated by adding IPA and FFA. As shown in Figure 5, the O/C of both 200 and 1000 nm PS decreased with the addition of IPA in solutions containing SRFA. This indicates that the generated $^\bullet$OH was involved in the oxidation of PS. The addition of FFA further decreased the O/C of PS compared with that in the presence of IPA, and the O/C (24 h of irradiation) of PS with particle sizes of 200 and 1000 nm decreased from 0.56 and 0.48 (in SRFA solution) to 0.11 and 0.14 (in SRFA solution with FFA), respectively. These results demonstrated that $^1O_2$ plays a major role in the oxidation of PS in SRFA solutions under simulated sunlight irradiation. As reported in a previous study, $^1O_2$ could induce the photooxidation of polymers with unsaturated alkenes, which leads to the formation of a carbonyl group.[59] Thus, the involvement of $^1O_2$ in the photodegradation of PS leads to an obvious increase in O/C.

As shown above, the adsorption of SRFA on PS occurs mainly through hydrophobic interactions to form heterogeneous aggregates in which PS can be regarded as a hydrophobic inner core. As a result, the hydrophobic components of SRFA directly interact with PS, forming a larger hydrophobic layer on the surface of PS. As proven by Latch and McNeill, the hydrophobic component of DOM contains more $^1O_2$ than $^1O_2$ in the aqueous phase.[60] Thus, it can be inferred that the enriched $^1O_2$ in the hydrophobic layer of SRFA and PS could react with PS, thereby leading to the fast oxidation of the surface of PS.

Generation of PPRIs from SRFA in the Presence of PS. The PPRIs generated from DOM in natural waters could induce the degradation of PS and increase the oxygen content on its surface. The concentrations of these PPRIs ($[PPRIs]_{ss}$) in the presence of PS in SRFA solutions were determined, and the results are shown in Tables 1 and S4. These results indicate that in SRFA solutions with a concentration of 10 mg/L, the concentrations of ^{3}SRFA* ($[^3SRFA^*]ss$), $^1O_2$ ($[^1O_2]ss$), and

https://doi.org/10.1021/acs.est.1c07129
Environ. Sci. Technol. 2022, 56, 3085−3095

Table 1. Steady-State Concentrations of the PPRIs ($[PPRIs]_{ss}$) from SRFA after 1 Week of Oscillation[a]

condition	$[^3DOM^*]_{SS}$ ($\times 10^{-13}$ M)	$[^1O_2]_{SS}$ ($\times 10^{-13}$ M)	$[^\bullet OH]_{SS}$ ($\times 10^{-17}$ M)
SRFA	4.53 ± 0.07	7.38 ± 0.01	4.78 ± 0.36
50 nm PS	2.46 ± 0.01	4.63 ± 0.09	3.02 ± 0.01
200 nm PS	3.28 ± 0.01	4.46 ± 0.01	2.01 ± 0.01
1000 nm PS	3.71 ± 0.01	4.68 ± 0.06	3.02 ± 0.71
SRFA + 0.5 mg/L PS	4.41 ± 0.03	5.07 ± 0.07	3.01 ± 0.01
SRFA + 5.0 mg/L PS	2.46 ± 0.01	4.63 ± 0.09	3.02 ± 0.01
SRFA + 10.0 mg/L PS	2.46 ± 0.01	4.23 ± 0.42	2.88 ± 0.12
SRFA + 20.0 mg/L PS	2.38 ± 0.02	3.46 ± 0.06	2.35 ± 0.01

[a]Oscillation conditions: 150 rpm, 25 °C; SRFA: 10 mg/L; PS: 20.0 mg/L for 50 nm, 200 nm, and 1000 nm; and PS: 50 nm with concentrations of 0.5, 5, 10, and 20 mg/L.

$^\bullet OH$ ($[^\bullet OH]ss$) were $(4.53 \pm 0.07) \times 10^{-13}$ M, $(7.38 \pm 0.01) \times 10^{-13}$ M, and $(4.78 \pm 0.36) \times 10^{-15}$ M, respectively.

In the presence of PS, the steady-state concentration of PPRIs did not change significantly during the direct irradiation process (Table S4). After oscillating for 1 week, the presence of PS significantly decreased the concentrations of these PPRIs (Table 1). With the coexistence of PS (50 nm), the $[^3DOM^*]ss$, $[^1O_2]ss$, and $[^\bullet OH]ss$ of SRFA decreased to $(2.38 \pm 0.07) \times 10^{-13}$ M, $(3.46 \pm 0.06) \times 10^{-13}$ M, and $(2.35 \pm 0.007) \times 10^{-15}$ M, respectively, as the concentration of PS increased from 0 to 20 mg/L (Table 1). Compared with $[^3DOM^*]ss$ and $[^\bullet OH]ss$, $[^1O_2]ss$ exhibited the lowest trend in the presence of 20 mg/L PS, with a decrease of 53.1% compared with that without PS. The decrease in $[PPRIs]_{ss}$ was supposed to be attributed to the inhibitory role of PS on the generation of these PPRIs or the promotional effect on the elimination of these PPRIs.

The role of PS in the elimination of these PPRIs could be confirmed by the increased content of O on the surface of PS (Figure 5). To verify the role of PS on the generation of PPRIs from DOM, the generation quantum yields of $^3DOM^*$ (Φ_{3DOM^*}), $^1O_2$ (Φ_{1O2}), and $^\bullet OH$ ($\Phi_{^\bullet OH}$) from SRFA under simulated sunlight irradiation were determined, and the results are shown in Figures 6 and S11. The results showed that the Φ_{3DOM^*}, Φ_{1O2}, and $\Phi_{^\bullet OH}$ of SRFA were $(1.32 \pm 0.02) \times 10^{-3}$, $(1.12 \pm 0.02) \times 10^{-3}$, and $(6.50 \pm 0.01) \times 10^{-5}$, respectively. These values are on the same order of magnitude as the values previously reported in the literature.[36,61] As shown in Figure S11, without oscillation, the presence of PS showed no obvious influence on the Φ_{3DOM^*}, Φ_{1O2}, and $\Phi_{^\bullet OH}$ of SRFA during direct irradiation. However, the Φ_{3DOM^*}, Φ_{1O2}, and $\Phi_{^\bullet OH}$ of SRFA decreased significantly in the presence of PS after oscillation for 1 week (Figure 6). Thus, it can be concluded that the presence of NPs in natural waters could affect the generation of PPRIs from DOM.

As shown in Table 1 and Figure 6, the effect of PS on the generation of PPRIs from SRFA is concentration-dependent. The concentrations and quantum yields of the PPRIs from SRFA decreased with the increase of the concentration of PS with a particle size of 50 nm, and sharp decreases were observed as the concentration of PS increased from 0 to 5 mg/L. Thus, the decrease in $[PPRIs]_{ss}$ in the presence of PS at lower concentrations (<5 mg/L) is mainly attributed to the inhibitory effect of PS on the generation of these PPRIs. Moreover, the addition of PS of different sizes also decreased the concentrations and Φ of these PPRIs from SRFA. Among the three PPRIs, the generation and elimination of $^1O_2$ from SRFA were mostly affected by PS. This is attributed to the accumulation of $^1O_2$ in the hydrophobic layer[60] and its reaction with PS at the hydrophobic interface of SRFA and PS.

Environmental Implications. The presence of NPs in the environment has attracted much concern due to their possible ecological risks. In natural waters, DOM has been proven to play an important role in the photodegradation of organic pollutants and in the transport of NPs. The results of this study showed that SRFA can enhance the aggregation of nanosized PS due to hydrophobic interactions. Thus, in natural waters, DOM could change the transport of NPs, and it is necessary to take the heteroaggregation induced by DOM into account for further fate modeling and risk assessment of NPs.

DOM not only induced the aggregation of NPs but was also able to enhance the oxidation of NPs. The generated $^3SRFA^*$, $^1O_2$, and $^\bullet OH$, especially $^1O_2$, from SRFA were proven to initiate the photooxidation of PS under simulated sunlight irradiation. These reactive species have been well proven to be present in sunlit surface waters, and their concentrations are on the same order as the determined values in this study.[62−64] Thus, these PPRIs could play an important role in the photoaging of plastics, especially plastics with small particle sizes. The oxidation of NPs leads to an increase in oxygen-containing functional groups on their surface, subsequently enhancing the hydrophilicity of NPs. This could promote their transport and transformation in natural waters. In addition, the increase in the oxygen content on the surface of NPs could also

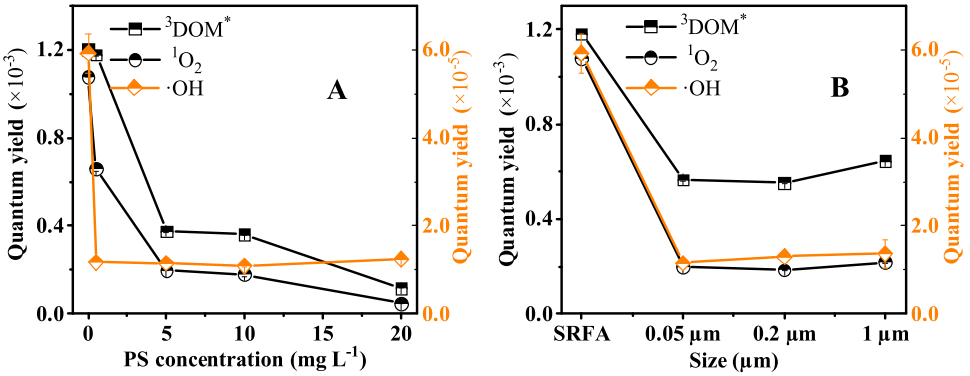

Figure 6. Quantum yield of PPRI generation from SRFA (10 mg/L) in the presence of PS (50 nm) at different concentrations (A) and of PS (20 mg/L) with different particle sizes (B). Oscillation conditions: 150 rpm, 25 °C; error bars for some data points are too small to be visible.

https://doi.org/10.1021/acs.est.1c07129
Environ. Sci. Technol. 2022, 56, 3085−3095

affect their bioavailability, as well as their interaction with either DOM or organic pollutants.

DOM in natural waters exhibits a great effect on the transport and transformation of NPs. In contrast, the presence of NPs could also affect the photochemical properties of DOM. As proven in this study, nanosized PS with concentrations higher than 0.5 mg/L significantly inhibited the generation of ^{3}SRFA*, $^1O_2$, and $^\bullet$OH from DOM under simulated sunlight irradiation, which led to a lower concentration of these oxidants in the SRFA solutions. In natural waters, floating plastics, especially NPs that are considered to have higher concentrations than MPs,[42] will change the concentration of these reactive species and thereafter influence the photodegradation of organic pollutants and the oxidation of other plastics.

■ ASSOCIATED CONTENT

Supporting Information

The Supporting Information is available free of charge at https://pubs.acs.org/doi/10.1021/acs.est.1c07129.

Calculation methods of quantum yield for reactive species; emission spectrum of a mercury lamp; SEM images of PS; average hydrodynamic diameter of PS; particle size distribution of PS; ζ-potentials of PS; average hydrodynamic diameter of PS in the presence of SRFA; particle size distribution of PS in the presence of SRFA; elemental composition (C and O) on the surface of PS; elemental composition (C and O) on the surface of PS during simulated sunlight irradiation; particle size distribution and average hydrodynamic diameters of PS during simulated sunlight irradiation; quantum yield of PPRIs from SRFA; analytical methods; parameters of the original PS particles; oxidation rate constants of PS; and steady-state concentrations of PPRIs from SRFA (PDF)

■ AUTHOR INFORMATION

Corresponding Author

Jiao Qu − *State Environmental Protection Key Laboratory of Wetland Ecology and Vegetation Restoration, School of Environment, Northeast Normal University, Changchun 130117, P. R. China;* orcid.org/0000-0001-6080-8704; Phone: +86-431-89165610; Email: quj100@nenu.edu.cn

Authors

Ya-nan Zhang − *State Environmental Protection Key Laboratory of Wetland Ecology and Vegetation Restoration, School of Environment, Northeast Normal University, Changchun 130117, P. R. China;* orcid.org/0000-0001-9792-0935

Fangyuan Cheng − *State Environmental Protection Key Laboratory of Wetland Ecology and Vegetation Restoration, School of Environment, Northeast Normal University, Changchun 130117, P. R. China*

Tingting Zhang − *State Environmental Protection Key Laboratory of Wetland Ecology and Vegetation Restoration, School of Environment, Northeast Normal University, Changchun 130117, P. R. China*

Chao Li − *State Environmental Protection Key Laboratory of Wetland Ecology and Vegetation Restoration, School of Environment, Northeast Normal University, Changchun 130117, P. R. China;* orcid.org/0000-0001-5523-0418

Jingwen Chen − *Key Laboratory of Industrial Ecology and Environmental Engineering (MOE), School of Environmental Science and Technology, Dalian University of Technology, Dalian 116024, P. R. China;* orcid.org/0000-0002-5756-3336

Willie J. G. M. Peijnenburg − *Institute of Environmental Sciences, Leiden University, Leiden 2300 RA, The Netherlands; National Institute of Public Health and the Environment (RIVM), Center for Safety of Substances and Products, Bilthoven 3720 BA, The Netherlands*

Complete contact information is available at: https://pubs.acs.org/10.1021/acs.est.1c07129

Notes

The authors declare no competing financial interest.

■ ACKNOWLEDGMENTS

This work was supported by the National Natural Science Foundation of China (Nos. 22176030, 42130705, 41877364, and 21976027), the Fundamental Research Funds for the Central Universities (Nos. 2412020FZ015 and 2412019FZ019), and the Jilin Province Science and Technology Development Projects (Nos. 20190303068SF and 20200301012RQ).

■ REFERENCES

(1) Law, K.; Thompson, R. Oceans. Microplastics in the seas. *Science* **2014**, *345*, 144−145.

(2) Napper, I. E.; Bakir, A.; Rowland, S. J.; Thompson, R. C. Characterisation, quantity and sorptive properties of microplastics extracted from cosmetics. *Mar. Pollut. Bull.* **2015**, *99*, 178−185.

(3) Rochman, C. Microplastics research—from sink to source. *Science* **2018**, *360*, 28−29.

(4) Thompson, R.; Olsen, Y.; Mitchell, R.; Davis, A.; Rowland, S.; John, A.; McGonigle, D. F.; Russell, A. Lost at sea: Where is all the plastic? *Science* **2004**, *304*, No. 838.

(5) Chae, Y.; An, Y.-J. Effects of micro- and nanoplastics on aquatic ecosystems: Current research trends and perspectives. *Mar. Pollut. Bull.* **2017**, *124*, 624−632.

(6) Koelmans, A. A.; Mohamed Nor, N. H.; Hermsen, E.; Kooi, M.; Mintenig, S. M.; De France, J. Microplastics in freshwaters and drinking water: Critical review and assessment of data quality. *Water Res.* **2019**, *155*, 410−422.

(7) Strungaru, S.-A.; Jijie, R.; Nicoara, M.; Plavan, G.; Faggio, C. Micro- (nano) plastics in freshwater ecosystems: Abundance, toxicological impact and quantification methodology. *TrAC, Trends Anal. Chem.* **2019**, *110*, 116−128.

(8) Li, C.; Gan, Y.; Zhang, C.; He, H.; Fang, J.; Wang, L.; Wang, Y.; Liu, J. "Microplastic communities" in different environments: Differences, links, and role of diversity index in source analysis. *Water Res.* **2021**, *188*, No. 116574.

(9) Wang, F.; Wong, C. S.; Chen, D.; Lu, X.; Wang, F.; Zeng, E. Y. Interaction of toxic chemicals with microplastics: A critical review. *Water Res.* **2018**, *139*, 208−219.

(10) Hu, K.; Tian, W.; Yang, Y.; Nie, G.; Zhou, P.; Wang, Y.; Duan, X.; Wang, S. Microplastics remediation in aqueous systems: Strategies and technologies. *Water Res.* **2021**, *198*, No. 117144.

(11) Vethaak, A. D.; Legler, J. Microplastics and human health. *Science* **2021**, *371*, 672−674.

(12) von Moos, N.; Burkhardt-Holm, P.; Köhler, A. Uptake and effects of microplastics on cells and tissue of the *Blue Mussel Mytilus edulis L.* after an experimental exposure. *Environ. Sci. Technol.* **2012**, *46*, 11327−11335.

(13) Velzeboer, I.; Kwadijk, C. J. A. F.; Koelmans, A. A. Strong sorption of PCBs to nanoplastics, microplastics, carbon nanotubes, and fullerenes. *Environ. Sci. Technol.* **2014**, *48*, 4869−4876.

(14) Zhan, Z.; Wang, J.; Peng, J.; Xie, Q.; Huang, Y.; Gao, Y. Sorption of 3,3′,4,4′-tetrachlorobiphenyl by microplastics: A case study of polypropylene. *Mar. Pollut. Bull.* **2016**, *110*, 559−563.
(15) Gauquie, J.; Devriese, L.; Robbens, J.; De Witte, B. A qualitative screening and quantitative measurement of organic contaminants on different types of marine plastic debris. *Chemosphere* **2015**, *138*, 348−356.
(16) Wang, F.; Shih, K. M.; Li, X. Y. The partition behavior of perfluorooctanesulfonate (PFOS) and perfluorooctanesulfonamide (FOSA) on microplastics. *Chemosphere* **2015**, *119*, 841−847.
(17) Zhao, M.; Zhang, T.; Yang, X.; Liu, X.; Zhu, D.; Chen, W. Sulfide induces physical damages and chemical transformation of microplastics via radical oxidation and sulfide addition. *Water Res.* **2021**, *197*, No. 117100.
(18) Chen, Q.; Wang, Q.; Zhang, C.; Zhang, J.; Dong, Z.; Xu, Q. Aging simulation of thin-film plastics in different environments to examine the formation of microplastic. *Water Res.* **2021**, *202*, No. 117462.
(19) Gardette, M.; Perthue, A.; Gardette, J.-L.; Janecska, T.; Földes, E.; Pukánszky, B.; Therias, S. Photo- and thermal-oxidation of polyethylene: Comparison of mechanisms and influence of unsaturation content. *Polym. Degrad. Stab.* **2013**, *98*, 2383−2390.
(20) Dawson, A. L.; Kawaguchi, S.; King, C. K.; Townsend, K. A.; King, R.; Huston, W. M.; Bengtson Nash, S. M. Turning microplastics into nanoplastics through digestive fragmentation by Antarctic krill. *Nat. Commun.* **2018**, *9*, No. 1001.
(21) Bouwmeester, H.; Hollman, P. C. H.; Peters, R. J. B. Potential health impact of environmentally released micro- and nanoplastics in the human food production chain: Experiences from nanotoxicology. *Environ. Sci. Technol.* **2015**, *49*, 8932−8947.
(22) Cai, L.; Hu, L.; Shi, H.; Ye, J.; Zhang, Y.; Kim, H. Effects of inorganic ions and natural organic matter on the aggregation of nanoplastics. *Chemosphere* **2018**, *197*, 142−151.
(23) Hüffer, T.; Praetorius, A.; Wagner, S.; von der Kammer, F.; Hofmann, T. Microplastic exposure assessment in aquatic environments: Learning from similarities and differences to engineered nanoparticles. *Environ. Sci. Technol.* **2017**, *51*, 2499−2507.
(24) Chen, W.; Ouyang, Z.-Y.; Qian, C.; Yu, H.-Q. Induced structural changes of humic acid by exposure of polystyrene microplastics: A spectroscopic insight. *Environ. Pollut.* **2018**, *233*, 1−7.
(25) Oriekhova, O.; Stoll, S. Heteroaggregation of nanoplastic particles in the presence of inorganic colloids and natural organic matter. *Environ. Sci.: Nano* **2018**, *5*, 792−799.
(26) Zhu, K.; Jia, H.; Sun, Y.; Dai, Y.; Zhang, C.; Guo, X.; Wang, T.; Zhu, L. Long-term phototransformation of microplastics under simulated sunlight irradiation in aquatic environments: Roles of reactive oxygen species. *Water Res.* **2020**, *173*, No. 115564.
(27) Wu, X.; Liu, P.; Wang, H.; Huang, H.; Shi, Y.; Yang, C.; Gao, S. Photo aging of polypropylene microplastics in estuary water and coastal seawater: Important role of chlorine ion. *Water Res.* **2021**, *202*, No. 117396.
(28) Guo, X.; Wang, J. The chemical behaviors of microplastics in marine environment: A review. *Mar. Pollut. Bull.* **2019**, *142*, 1−14.
(29) Liu, P.; Qian, L.; Wang, H.; Zhan, X.; Lu, K.; Gu, C.; Gao, S. New insights into the aging behavior of microplastics accelerated by advanced oxidation processes. *Environ. Sci. Technol.* **2019**, *53*, 3579−3588.
(30) Liu, Y.; Hu, Y.; Yang, C.; Chen, C.; Huang, W.; Dang, Z. Aggregation kinetics of UV irradiated nanoplastics in aquatic environments. *Water Res.* **2019**, *163*, No. 114870.
(31) Müller, A.; Becker, R.; Dorgerloh, U.; Simon, F.-G.; Braun, U. The effect of polymer aging on the uptake of fuel aromatics and ethers by microplastics. *Environ. Pollut.* **2018**, *240*, 639−646.
(32) Mao, Y.; Li, H.; Huangfu, X.; Liu, Y.; He, Q. Nanoplastics display strong stability in aqueous environments: Insights from aggregation behaviour and theoretical calculations. *Environ. Pollut.* **2020**, *258*, No. 113760.
(33) Wang, H.; Liu, P.; Wang, M.; Wu, X.; Shi, Y.; Huang, H.; Gao, S. Enhanced phototransformation of atorvastatin by polystyrene microplastics: Critical role of aging. *J. Hazard. Mater.* **2021**, *408*, No. 124756.
(34) Zhang, Y.; Wang, J.; Chen, J.; Zhou, C.; Xie, Q. Phototransformation of 2,3-dibromopropyl-2,4,6-tribromophenyl ether (DPTE) in natural waters: Important roles of dissolved organic matter and chloride ion. *Environ. Sci. Technol.* **2018**, *52*, 10490−10499.
(35) McNeill, K.; Canonica, S. Triplet state dissolved organic matter in aquatic photochemistry: Reaction mechanisms, substrate scope, and photophysical properties. *Environ. Sci.: Processes Impacts* **2016**, *18*, 1381−1399.
(36) Zhou, Y.; Cheng, F.; He, D.; Zhang, Y.; Qu, J.; Yang, X.; Chen, J.; Peijnenburg, W. J. G. M. Effect of UV/chlorine treatment on photophysical and photochemical properties of dissolved organic matter. *Water Res.* **2021**, *192*, No. 116857.
(37) Rosario-Ortiz, F. L.; Canonica, S. Probe compounds to assess the photochemical activity of dissolved organic matter. *Environ. Sci. Technol.* **2016**, *50*, 12532−12547.
(38) Chen, C.-S.; Le, C.; Chiu, M.-H.; Chin, W.-C. The impact of nanoplastics on marine dissolved organic matter assembly. *Sci. Total Environ.* **2018**, *634*, 316−320.
(39) Dalrymple, R. M.; Carfagno, A. K.; Sharpless, C. M. Correlations between dissolved organic matter optical properties and quantum yields of singlet oxygen and hydrogen peroxide. *Environ. Sci. Technol.* **2010**, *44*, 5824−5829.
(40) Guaita, M.; Chiantore, O.; Costa, L. Changes in degree of polymerization in the thermal degradation of polystyrene. *Polym. Degrad. Stab.* **1985**, *12*, 315−332.
(41) Lenz, R.; Enders, K.; Nielsen, T. G. Microplastic exposure studies should be environmentally realistic. *Proc. Natl. Acad. Sci. U.S.A.* **2016**, *113*, E4121−E4122.
(42) Besseling, E.; Redondo-Hasselerharm, P.; Foekema, E. M.; Koelmans, A. A. Quantifying ecological risks of aquatic micro- and nanoplastic. *Crit. Rev. Environ. Sci. Technol.* **2019**, *49*, 32−80.
(43) Cheng, F.; He, J.; Li, C.; Lu, Y.; Zhang, Y.; Qu, J. Photo-induced degradation and toxicity change of decabromobiphenyl ethers (BDE-209) in water: Effects of dissolved organic matter and halide ions. *J. Hazard. Mater.* **2021**, *416*, No. 125842.
(44) Grebel, J. E.; Pignatello, J. J.; Mitch, W. A. Sorbic acid as a quantitative probe for the formation, scavenging and steady-state concentrations of the triplet-excited state of organic compounds. *Water Res.* **2011**, *45*, 6535−6544.
(45) Fan, J.; Qin, H.; Jiang, S. Mn-doped g-C3N4 composite to activate peroxymonosulfate for acetaminophen degradation: The role of superoxide anion and singlet oxygen. *Chem. Eng. J.* **2019**, *359*, 723−732.
(46) Latch, D. E.; Stender, B. L.; Packer, J. L.; Arnold, W. A.; McNeill, K. Photochemical fate of pharmaceuticals in the environment: Cimetidine and ranitidine. *Environ. Sci. Technol.* **2003**, *37*, 3342−3350.
(47) Mostafa, S.; Rosario-Ortiz, F. Singlet oxygen formation from wastewater organic matter. *Environ. Sci. Technol.* **2013**, *47*, 8179−8186.
(48) Glover, C. M.; Rosario-Ortiz, F. L. Impact of halides on the photoproduction of reactive intermediates from organic matter. *Environ. Sci. Technol.* **2013**, *47*, 13949−13956.
(49) McKay, G.; Rosario-Ortiz, F. L. Temperature dependence of the photochemical formation of hydroxyl radical from dissolved organic matter. *Environ. Sci. Technol.* **2015**, *49*, 4147−4154.
(50) Zhou, H.; Yan, S.; Lian, L.; Song, W. Triplet-State photochemistry of dissolved organic matter: Triplet-State energy distribution and surface electric charge conditions. *Environ. Sci. Technol.* **2019**, *53*, 2482−2490.
(51) Wu, J.; Jiang, R.; Lin, W.; Ouyang, G. Effect of salinity and humic acid on the aggregation and toxicity of polystyrene nanoplastics with different functional groups and charges. *Environ. Pollut.* **2019**, *245*, 836−843.

https://doi.org/10.1021/acs.est.1c07129
Environ. Sci. Technol. 2022, 56, 3085−3095

(52) Wu, X.; Liu, P.; Shi, H.; Wang, H.; Huang, H.; Shi, Y.; Gao, S. Photo aging and fragmentation of polypropylene food packaging materials in artificial seawater. *Water Res.* **2021**, *188*, No. 116456.
(53) Chen, W.; Westerhoff, P.; Leenheer, J. A.; Booksh, K. Fluorescence excitation−emission matrix regional integration to quantify spectra for dissolved organic matter. *Environ. Sci. Technol.* **2003**, *37*, 5701−5710.
(54) Sharpless, C. M.; Blough, N. V. The importance of charge-transfer interactions in determining chromophoric dissolved organic matter (CDOM) optical and photochemical properties. *Environ. Sci.: Processes Impacts* **2014**, *16*, 654−671.
(55) Ma, J.; Del Vecchio, R.; Golanoski, K. S.; Boyle, E. S.; Blough, N. V. Optical properties of humic substances and CDOM: Effects of borohydride reduction. *Environ. Sci. Technol.* **2010**, *44*, 5395−5402.
(56) Zhang, D.; Yan, S.; Song, W. Photochemically induced formation of reactive oxygen species (ROS) from effluent organic matter. *Environ. Sci. Technol.* **2014**, *48*, 12645−12653.
(57) Zhu, K.; Jia, H.; Zhao, S.; Xia, T.; Guo, X.; Wang, T.; Zhu, L. Formation of environmentally persistent free radicals on microplastics under light irradiation. *Environ. Sci. Technol.* **2019**, *53*, 8177−8186.
(58) Wang, C.; Xian, Z.; Jin, X.; Liang, S.; Chen, Z.; Pan, B.; Wu, B.; Ok, Y. S.; Gu, C. Photo-aging of polyvinyl chloride microplastic in the presence of natural organic acids. *Water Res.* **2020**, *183*, No. 116082.
(59) Yousif, E.; Haddad, R. Photodegradation and photostabilization of polymers, especially polystyrene: review. *SpringerPlus* **2013**, *2*, No. 398.
(60) Latch, D. E.; McNeill, K. Microheterogeneity of singlet oxygen distributions in irradiated humic acid solutions. *Science* **2006**, *311*, 1743−1747.
(61) Wang, J.; Chen, J.; Qiao, X.; Zhang, Y.; Uddin, M.; Guo, Z. Disparate effects of DOM extracted from coastal seawaters and freshwaters on photodegradation of 2,4-dihydroxybenzophenone. *Water Res.* **2019**, *151*, 280−287.
(62) Zepp, R. G.; Schlotzhauer, P. F.; Sink, R. M. Photosensitized transformations involving electronic energy transfer in natural waters: Role of humic substances. *Environ. Sci. Technol.* **1985**, *19*, 74−81.
(63) Haag, W.; Hoigne, J. Singlet oxygen in surface waters. 3. Photochemical formation and steady-state concentrations in various types of waters. *Environ. Sci. Technol.* **1986**, *20*, 341−348.
(64) Mopper, K.; Zhou, X. Hydroxyl radical photoproduction in the sea and its potential impact on marine processes. *Science* **1990**, *250*, 661−664.

https://doi.org/10.1021/acs.est.1c07129
Environ. Sci. Technol. 2022, 56, 3085−3095